

Experimental Separation of Virtual Photon Exchange and Electron Transfer in Interatomic Coulombic Decay of Neon Dimers

T. Jahnke,^{1,*} A. Czasch,¹ M. Schöffler,¹ S. Schössler,¹ M. Kász,¹ J. Titze,¹ K. Kreidi,⁵ R. E. Grisenti,¹ A. Staudte,² O. Jagutzki,¹ L. Ph. H. Schmidt,¹ Th. Weber,³ H. Schmidt-Böcking,¹ K. Ueda,⁴ and R. Dörner¹

¹*Institut für Kernphysik, J. W. Goethe-Universität Frankfurt am Main, Max-von-Laue-Str. 1, D-60438 Frankfurt, Germany*

²*Steacie Institute for Molecular Sciences, 100 Sussex Drive, Ottawa, Canada*

³*Lawrence Berkeley National Laboratory, Berkeley California 94720, USA*

⁴*Institute of Multidisciplinary Research for Advanced Materials, Tohoku University, Sendai 980-8577, Japan*

⁵*DESY, Notkestrasse 85, 22607 Hamburg, Germany*

(Received 21 June 2007; published 12 October 2007)

We investigate the interatomic Coulombic decay (ICD) of neon dimers following photoionization with simultaneous excitation of the ionized atom (shakeup) in a multiparticle coincidence experiment. We find that, depending on the parity of the excited state, which determines whether ICD takes place via virtual dipole photon emission or overlap of the wave functions, the decay happens at different internuclear distances, illustrating that nuclear dynamics heavily influence the electronic decay in the neon dimer.

DOI: 10.1103/PhysRevLett.99.153401

PACS numbers: 36.40.Mr, 33.80.Eh, 34.30.+h, 82.33.Fg

Until about ten years ago, it was assumed that the chemical environment of an atom does not dramatically affect its decay dynamics. In 1997, Cederbaum *et al.* showed that this is not true for some van der Waals or hydrogen bound systems [1]; a phenomenon termed “Interatomic Coulombic Decay” (ICD) was proposed. As ICD occurs, the energy of an excited atom in van der Waals or hydrogen bound matter is used to release a low energy electron from a *neighboring* atom. During the last three years, the existence of ICD has been proven experimentally by means of electron spectroscopy [2] and multiparticle coincidence momentum spectroscopy techniques (COLTRIMS) [3]. Later experimental evidence of ICD in species other than a neon cluster was found, as well [4].

Extensive theoretical work has been carried out on ICD in neon clusters [5–10] and many other species [1,11]. For the case of ICD after $2s$ photoionization in neon dimers, the decay rate is proportional to $|V_{L2p,R2p,L2s,k} - V_{L2p,R2p,k,L2s}|^2$, where the two electron-electron Coulomb matrix elements

$$V_{L2p,R2p,L2s,k} = \iint \phi_{L2p}^*(\vec{r}_1) \phi_{L2s}(\vec{r}_1) \times \frac{e^2}{|\vec{r}_1 - \vec{r}_2|} \phi_{R2p}^*(\vec{r}_2) \phi_k(\vec{r}_2) d\vec{r}_1 d\vec{r}_2 \quad (1)$$

and

$$V_{L2p,R2p,k,L2s} = \iint \phi_{L2p}^*(\vec{r}_1) \phi_k(\vec{r}_1) \times \frac{e^2}{|\vec{r}_1 - \vec{r}_2|} \phi_{R2p}^*(\vec{r}_2) \phi_{L2s}(\vec{r}_2) d\vec{r}_1 d\vec{r}_2 \quad (2)$$

are denoted as “direct” and “exchange” contribution, respectively [6,12]. These two matrix elements are schematically illustrated in Fig. 1. The indices of the wave

functions in Eqs. (1) and (2) are chosen according to Fig. 1 with “ R ” denoting an orbital from the “right” neon atom and “ L ” one from the left atom of the dimer. The notations “ $2s$ ” and “ $2p$ ” describe the involved shells, and “ k ” refers to the continuum photoelectron. The description given above looks identical to that of an Auger decay, where the two contributions $V_{L2p,R2p,L2s,k}$ and $V_{L2p,R2p,k,L2s}$ arise from the simple fact that the electrons that are involved in the decay are indistinguishable. An essential difference occurs when the participating electrons are located at two different atoms, as in the case of ICD in a neon dimer. The *direct* integral [Eq. (1)] describes the case in which a $2p$ electron of the same atom drops into the previously created $2s$ hole and a $2p$ electron from the other atom of the dimer is emitted. [See Fig. 1(a), left pathway.] The *exchange* integral [Eq. (2)] describes a process of electron transfer: the $2s$ hole at the left neon atom is filled by a $2p$ electron from the right atom, leading to the emission of another $2p$ electron from the left atom. [See Fig. 1(a), right pathway]. The contributions from these two integrals to the decay rates depend very differently on the internuclear distance R of the involved atoms [12,13]. The exchange integral requires some overlap of the two wave functions, and thus the decay rate exponentially decreases with increasing R , whereas the direct term decreases more gently and survives at large R where the overlap of the wave function is negligible [6]. The direct integral of Eq. (1) may alternatively be called “virtual photon exchange” in contrast to the “electron exchange” of Eq. (2) [13]: the $2s$ hole in the left atom is filled with a $2p$ electron in the same atom by the *virtual* photon emission, and a $2p$ electron in the right atom is ejected by the *virtual* photon absorption. The ICD rate due to this virtual photon exchange is proportional to $1/R^6$ at large internuclear distances [13].

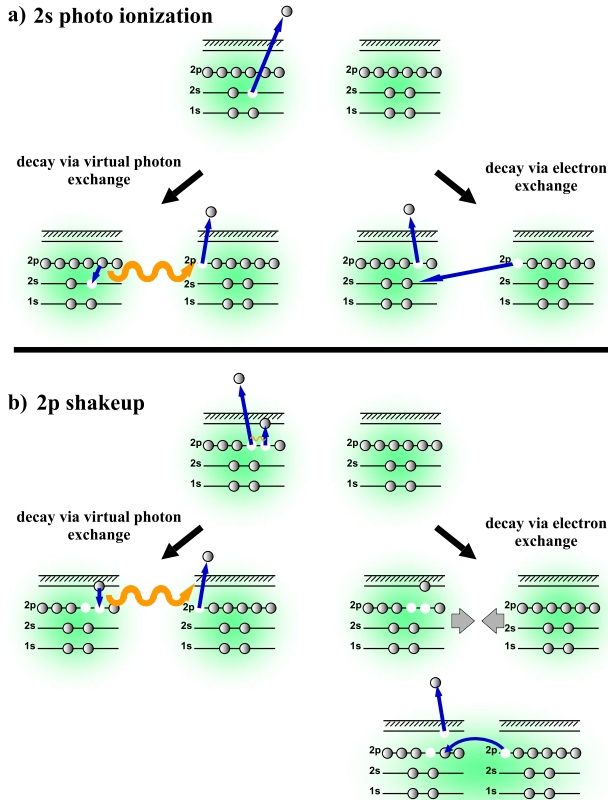


FIG. 1 (color online). (a) Two possible paths of decay in a neon dimer after creation of a $2s$ hole (adapted from [6]). Left pathway: a virtual photon is transferred between the two atoms of the dimer, leading to the emission of a $2p$ electron of the right atom. Right pathway: competing process in which an electron is transferred leading to the emission of a $2p$. (b) Corresponding process after population of $2p$ shakeup states, which is investigated in the present experiment.

In the present Letter, instead of examining decay after $2s$ ionization as shown in Fig. 1(a), we investigate decay from different shakeup states created by photoemission of a $2s$ electron with simultaneous excitation of another $2p$ electron, as depicted in Fig. 1(b). Our expectation is the following. Shakeup states of *even* parity—just like the $2s$ ionized state investigated so far [2,3]—can decay to the $2p$ ionized ground state via virtual *dipole* photon emission (i.e., the dipole-allowed virtual photon exchange ICD channel is open), whereas decay from excited states of *odd* parity to the ionized ground state is dipole forbidden, and thus the ICD takes place only at small R where the overlap of the orbitals becomes significant. Measuring R at the instance of ICD by detecting the kinetic energy release (KER) for each shakeup state separately, we have successfully demonstrated that the *dipole-allowed* ICD takes place at the instant of photoionization at the equilibrium R of the ground state, whereas the *dipole-forbidden* ICD takes place only after shortening of R , i.e., contraction of the dimer.

Our experiment has been performed at beam line U125/1-PGM of the BESSY II synchrotron radiation facility in Berlin in single bunch operation using the COLTRIMS (COLd Target Recoil Ion Momentum Spectroscopy) technique [14–16]. In brief, a supersonic jet is crossed with the photon beam from the synchrotron, thus creating a well-defined target region of approximately $0.5 \times 0.5 \times 3 \text{ mm}^3$. Homogenous electric and magnetic fields are used to guide charged fragments created in a photo reaction to two position and time sensitive microchannel plate detectors with delayline position readout [17,18]. By measuring the time of flight and the position of impact on the detector, the initial vector momentum of each particle is obtained during offline analysis. The guiding fields ($E = 5.4 \text{ V/cm}$ and $B = 7 \text{ Gauss}$, respectively) were chosen such that electrons with an initial kinetic energy of up to 12 eV and ions with an energy of up to 4 eV are detected in coincidence with a solid angle of emission of 4π . On the electron arm of the spectrometer, a field free drift region is introduced in order to employ McLaren-time focussing [19]. A triple coincidence condition requiring detection of two singly charged ions and at least one electron was used during data acquisition in order to suppress events originating from monomer and residual gas ionization. In about 10% of the recorded data, all four particles from the complete dimer breakup were detected in coincidence. Furthermore, during offline analysis, valid events of a neon dimer breaking up after photoionization were identified by checking for momentum conservation of the two ions: as the dimer fragments in a Coulomb explosion, the ions' momenta have to be equal in magnitude and directed oppositely.

In [3], the key figure [Fig. 4(a)] showed the measured electron energy in dependence of the KER of the Coulomb exploding dimer. Events of ICD were identified as a diagonal line in that representation of the data. Figure 2(a) shows that distribution on a logarithmic color scale. Apart from the structures described in [3], a set of new features appears at higher KERs and photo electron energies that do not belong to ICD or $2s$ photoionization. In order to identify the origin of those features, Fig. 2(b) shows the sum of all particles' kinetic energies for the case that all four particles (two neon ions and two electrons) were detected in quadruple coincidence. It peaks at a value of 15.6 eV for all KERs observed. Energy conservation requires that

$$E_1 + E_2 + \text{KER} = h\nu - 2\text{IP}(\text{Ne}^+), \quad (3)$$

where $h\nu = 58.8 \text{ eV}$ is the photon energy. $E_1 + E_2 + \text{KER} = 15.6 \text{ eV}$ in Fig. 2(b) thus corresponds to an ionization potential $\text{IP} = 21.6 \text{ eV}$ which is the energy needed to ionize a $2p$ electron of a Ne atom with the singly charged ion remaining in its ground state.

We now show that all features in Fig. 2(a) besides A and B (see figure caption for explanation) result from ICD following $2p$ ionization plus excitation of one of the Ne

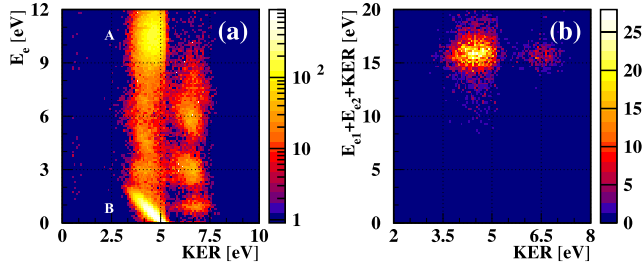


FIG. 2 (color online). (a) The measured electron energy E_e and kinetic energy of the ions KER on a logarithmic color scale. Clearly visible are the features corresponding to ICD after $2s$ ionization: the peak of $2s$ photoelectron (A) and the diagonal line belonging to the detected ICD electrons (B). Furthermore, some features at higher KERs and different photo electron energies are visible. (b) Total measured kinetic energy ($E_{e1} + E_{e2} + \text{KER}$) of the four particle breakup of the dimer in dependence of the KER. The graph shows that for all events shown in (a), the sum kinetic energy is, within the experiment's resolution, 15.6 eV, thus showing that the photo ions are not electronically excited in their final state and no energy was lost, e.g., by emission of a photon during the process.

atoms. Shakeup states of single neon atoms have been studied in a wide range of photon energies (e.g., [20–22]). Previous work in a photon energy region below 85 eV (thus being suitable for comparisons with our measurements) can be found in [23]. A large amount of satellite-states of the type $\text{Ne}(2s^2 2p^4 nl)$ are observed for binding energies in a region from the $2s$ -threshold to 65 eV. A comparison of that distribution with our data is shown in Fig. 3. The distribution shown in Fig. 3 (bottom) is the same as the one in Fig. 2(a) but on a linear color scale with the intensity being cropped at 55 counts in order to enhance the visibility of events that do not belong to the strongly dominating $2s$ photoionization and its corresponding ICD. In addition to all lines of the monomer appearing in [23], our data on the dimer show some additional features such as, for example, a prominent structure at a KER of ~ 4.5 eV and an electron energy of ~ 4.5 eV (labeled “D2”). They result from interatomic decay of shakeup states. The total sum kinetic energy that is available is 15.6 eV. Thus, for a KER of 4.5 eV, an energy of 11.1 eV can be shared between the photo (shakeup) electron and the second electron emitted. Every shakeup line has to have a corresponding second feature in our plot which is located at an energy of $15.6 \text{ eV} - \text{KER} - E_{e1}$. In most of the cases, those overlap in part with other shakeup lines but, for example, electrons belonging to $\text{Ne}(2s^2 2p^4 3s)$ (“D1”) are the ones depicted as “D2.” Features belonging together are labeled in Fig. 3 with the same letter, with the shakeup line being marked as “1” and the electron from interatomic decay as “2.”

A major feature is, however, that different states group in two distinct regions of KER. For a diatomic system fragmenting in a Coulomb explosion, the KER depends on the

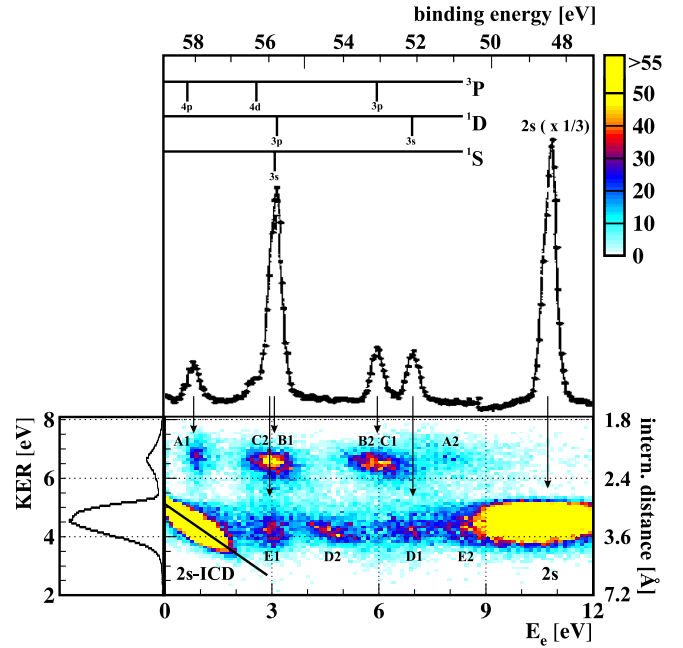


FIG. 3 (color online). The distribution of shakeup lines from [23] (top) in comparison with our results (bottom). Our results show the electron energy in dependence of the KER; the KER-distribution itself is shown on the left. The internuclear distance according to Eq. (4) is depicted on the right. Pairs of features belonging to a shakeup state and its corresponding second electron from interatomic decay are labeled with the same letters followed by 1 (for the shakeup line) or “2” (for the corresponding second electron). Shakeup states with even parity appear close to the mean internuclear distance of the dimer's ground state of $R = 3.3 \text{ \AA}$. Shakeup states of odd parity appear at a higher KER > 5.5 eV, i.e., at smaller internuclear distances.

internuclear distance R of the two ions at the time the Coulomb explosion is initiated. For a pure Coulomb potential, which is a reasonable approximation for the large internuclear separations relevant here, one obtains [24]:

$$R = \frac{q_1 q_2}{4\pi\epsilon_0 E_{\text{KER}}}, \quad (4)$$

where R is the internuclear distance at the instance of decay. Correspondingly, the measured internuclear distance is shown on the right hand side of Fig. 3 shows that some states decay close to the mean internuclear distance of the dimer of 3.2 \AA [25] (corresponding to a KER of 4.5 eV), others at a much smaller internuclear distance $< 2.6 \text{ \AA}$ (KER > 5.5 eV). The reason for this behavior can be found when examining the configuration of the shakeup states in more detail: the Ne^+ ground state is of odd parity. In an ICD-like process where the energy is transferred via virtual photon exchange, the parity of the ion state needs to flip due to the angular momentum of the emitted virtual photon. It appears that all shakeup states of even parity decay at the mean internuclear distance close to that of the dimer ground state, while all states of odd parity

decay at much smaller distances. These data directly show that if the excited neon atom is in a state that can decay in a dipole transition to the ground state, the process happens in the same short time scale as for “normal” ICD after $2s$ ionization, thus with the atoms of the dimer being at an internuclear distance close to that of the initial ground state. If, on the other hand, the dimer was excited to a state whose decay is dipole forbidden, the Ne_2^+ is metastable at this internuclear distance. It starts to contract following the Ne_2^+ potential energy curve which, obviously, has a minimum at much smaller R than the neutral Ne_2 . As soon as the electron orbitals of the two neon atoms have sufficient overlap, the ICD takes place; as in this case, a flip of parity is not necessary. Therefore, in the case of odd shakeup states, the kinetic energy of the ions reveal at what internuclear distance the overlap becomes significant, allowing for a decay involving electron transfer.

In summary, we used COLTRIMS to investigate the decay of neon dimers after ionization with photons of 58.8 eV energy. The multicoincidence measurement reveals the existence of an interatomic decay that occurs after the population of shakeup states. As the parity of the excited state determines whether ICD takes place due to virtual dipole photon emission or overlap of the orbitals, the decay happens at different internuclear distances leading to different kinetic energies of the ions. Electron exchange that happens only via overlap of the orbitals is strongly suppressed compared to virtual dipole photon exchange at the equilibrium internuclear distance of the neon dimer. Similar to the case of doubly excited states [26], the nuclear dynamics heavily influence the electronic decay pathways in the Ne dimer. In turn, imaging this dynamics in coincidence with the electrons unveils the physical mechanism underlying the electronic transitions.

We would like to thank U. Hergenhahn for his support during the measurement and discussions afterwards. Furthermore, we would like to express our thanks to L. Cederbaum and the entire Cederbaum group, especially S. Scheit and V. Averbukh, for the great support from the side of theory. This work was supported by the Berliner Elektronen Speicherring für Synchrotronstrahlung (BESSY), BMBF, Alexander von Humboldt Foundation, and GSI.

*jahnke@atom.uni-frankfurt.de

- [1] L. S. Cederbaum, J. Zobeley, and F. Tarantelli, *Phys. Rev. Lett.* **79**, 4778 (1997).
- [2] S. Marburger, O. Kugeler, U. Hergenhahn, and T. Möller, *Phys. Rev. Lett.* **90**, 203401 (2003).
- [3] T. Jahnke, A. Czasch, M. S. Schöffler, S. Schössler, A. Knapp, M. Käs, J. Titze, C. Wimmer, K. Kreidi, R. E. Grisenti, A. Staudte, O. Jagutzki, U. Hergenhahn, H. Schmidt-Böcking, and R. Dörner, *Phys. Rev. Lett.* **93**, 163401 (2004).
- [4] Y. Morishita, X.-J. Liu, N. Saito, T. Lischke, M. Kato, G. Prümper, M. Oura, H. Yamaoka, Y. Tamenori, I. H. Suzuki, and K. Ueda, *Phys. Rev. Lett.* **96**, 243402 (2006).
- [5] R. Santra, J. Zobeley, L. S. Cederbaum, and N. Moiseyev, *Phys. Rev. Lett.* **85**, 4490 (2000).
- [6] R. Santra, J. Zobeley, and L. S. Cederbaum, *Phys. Rev. B* **64**, 245104 (2001).
- [7] N. Moiseyev, R. Santra, J. Zobeley, and L. S. Cederbaum, *J. Chem. Phys.* **114**, 7351 (2001).
- [8] R. Santra and L. S. Cederbaum, *Phys. Rev. Lett.* **90**, 153401 (2003).
- [9] S. Scheit, L. S. Cederbaum, and H.-D. Meyer, *J. Chem. Phys.* **118**, 2092 (2003).
- [10] S. Scheit, V. Averbukh, H.-D. Meyer, N. Moiseyev, R. Santra, T. Sommerfeld, J. Zobeley, and L. S. Cederbaum, *J. Chem. Phys.* **121**, 8393 (2004).
- [11] V. Averbukh and L. S. Cederbaum, *Phys. Rev. Lett.* **96**, 053401 (2006).
- [12] R. Santra and L. S. Cederbaum, *Phys. Rep.* **368**, 1 (2002).
- [13] V. Averbukh, I. B. Müller, and L. S. Cederbaum, *Phys. Rev. Lett.* **93**, 263002 (2004).
- [14] R. Dörner, V. Mergel, O. Jagutzki, L. Spielberger, J. Ullrich, R. Moshhammer, and H. Schmidt-Böcking, *Phys. Rep.* **330**, 95 (2000).
- [15] J. Ullrich, R. Moshhammer, A. Dorn, R. Dörner, L. Ph. H. Schmidt, and H. Schmidt-Böcking, *Rep. Prog. Phys.* **66**, 1463 (2003).
- [16] T. Jahnke, Th. Weber, T. Osipov, A. L. Landers, O. Jagutzki, L. Ph. H. Schmidt, C. L. Cocke, M. H. Prior, H. Schmidt-Böcking, and R. Dörner, *J. Electron Spectrosc. Relat. Phenom.* **141**, 229 (2004).
- [17] O. Jagutzki, V. Mergel, K. Ullmann-Pfleger, L. Spielberger, U. Spillmann, R. Dörner, and H. Schmidt-Böcking, *Nucl. Instrum. Methods Phys. Res., Sect. A* **477**, 244 (2002).
- [18] See <http://www.roentdek.com> for details on the detectors.
- [19] W. C. Wiley and I. H. McLaren, *Rev. Sci. Instrum.* **26**, 1150 (1955).
- [20] F. Wuilleumier and M. O. Krause, *Phys. Rev. A* **10**, 242 (1974).
- [21] U. Becker, R. Holzel, H. B. Kerkhoff, B. Langer, D. Szostak, and R. Wehlitz, *Phys. Rev. Lett.* **56**, 1120 (1986).
- [22] S. Svensson, B. Eriksson, N. Martensson, G. Wendin, and U. Gelius, *J. Electron Spectrosc. Relat. Phenom.* **47**, 327 (1988).
- [23] G. Kutluk, T. Takaku, M. Kanno, T. Nagata, E. Shigemasa, A. Yagishita, and F. Koike, *J. Phys. B* **27**, 5637 (1994).
- [24] T. Weber, A. Czasch, O. Jagutzki, A. K. Müller, V. Mergel, A. Kheifets, E. Rotenberg, G. Meigs, M. H. Prior, S. Daveau, A. Landers, C. L. Cocke, T. Osipov, R. Diez Muino, H. Schmidt-Böcking, and R. Dörner, *Nature (London)* **431**, 437 (2004).
- [25] A. Wüest and F. Merkt, *J. Chem. Phys.* **118**, 8807 (2003).
- [26] F. Martin, J. Fernandez, T. Havermeier, L. Foucar, Th. Weber, K. Kreidi, M. Schöffler, L. Schmidt, T. Jahnke, O. Jagutzki, A. Czasch, E. P. Benis, T. Osipov, A. L. Landers, A. Belkacem, M. H. Prior, H. Schmidt-Böcking, C. L. Cocke, and R. Dörner, *Science* **315**, 629 (2007).